

Exciting erbium-doped planar optical amplifier materials

A. Polman

FOM-Institute for Atomic and Molecular Physics
Kruislaan 407, 1098 SJ Amsterdam, The Netherlands

ABSTRACT

Erbium-doped planar optical amplifiers can find numerous applications in photonic integrated circuits operating at 1.5 μm . The challenge is to fabricate these devices with *high gain*, operating at *low pump power*, and having *small overall size*. In this paper a review is given of our recent work in the area of Er-doped waveguide materials and amplifiers based on three materials classes: *oxide films* (Al_2O_3 , Y_2O_3 , SiO_2), *polymers*, and *silicon*.

The smallest amplifier (1 mm^2), is made using Al_2O_3 channel waveguides and operates at a pump power of 10 mW, providing a gain of 2.3 dB. In this material a cooperative upconversion interaction between excited Er ions is the main gain-limiting factor. We show that Er-doped Al_2O_3 waveguides with similar Er concentration, but fabricated using different methods, can show completely different upconversion coefficients. In Y_2O_3 we show that Eu co-doping can increase the gain performance and reduce the influence of upconversion. In SiO_2 , sensitizers such as Yb ions or Si quantum dots enhance the pump efficiency. A precise optimization of the silica network composition has enabled the fabrication of an optical amplifier with a gain as high as 4.1 dB/cm.

Polymer waveguides can be doped with Er ions encapsulated in an organic cage complex. While the 1.5 μm emission bandwidth in these complexes is as large as 70 nm, the luminescence quantum efficiency is small, due to coupling to vibrational states. Sensitizers can be attached to the complex to increase the excitation rate. The quenching problem can be solved by using a nanocomposite material, in which the Er is incorporated in silica colloids that are embedded in the polymer.

Silicon is an excellent waveguide material at 1.5 μm , and it is a challenge to fabricate an electrically pumped optical amplifier in this material. Clear 1.5 μm luminescence can be observed from Er-doped single-crystal Si, but strong quenching is observed at room temperature due to a backtransfer process. We demonstrate that by taking advantage of the known nano-fabrication technology for Si, photonic crystal waveguides can be made with extremely small dimensions.

Keywords: erbium, ytterbium, europium, Al_2O_3 , SiO_2 , polymer, Si, quantum dot, organic complex, upconversion, sensitizer, waveguide, optical gain, planar optical amplifier, integrated optics, photonic crystal

1. INTRODUCTION

Erbium-doped materials are of great interest in optical communications technology, as they can serve as the gain medium in optical amplifiers operating at the standard telecommunications wavelength of 1.5 μm .^{1,2} Er^{3+} ions, when incorporated in a solid host, show well-defined energy levels of the 4f-shell electronic configurations (see Fig. 1(a)).³ The transition from the first excited state to the ground state ($^4\text{I}_{13/2} \rightarrow ^4\text{I}_{15/2}$) occurs at 1.53 μm and is being employed to provide the gain in optical fiber amplifiers in long-distance telecommunication links worldwide. Medium- and long-distance optical communication is by now well established. The next development will be the introduction of optical links on a local scale, denoted as fiber-to-the-home technology. For this to become a reality, it is essential that a technology for the processing of optical signals on a local scale is established. Planar photonic integrated circuits are being developed to perform functions such as guiding, splitting, switching, wavelength multiplexing and amplification of light. Figure 1(b) shows an example of the layout of such an optical chip, in which a variety of straight channel waveguides, waveguide bends and loops, splitters, and wavelength division multiplexers are integrated on one single chip with an area of 1 cm^2 . At present, many of the materials and device concepts for this planar technology are still in the development stage.

This paper will focus on one important component in planar integrated photonic circuits, i.e. the optical amplifier. Such a device can serve e.g. to compensate for coupling losses, waveguide losses, or the power division in optical splitters. As most planar waveguide devices are based on oxide materials or polymers, it appears of great interest to study the doping of such materials with erbium and to investigate the optical gain characteristics and perspectives.⁴ This paper will also discuss the use of silicon as a planar waveguide material, in which both the guiding and semiconducting properties are combined.

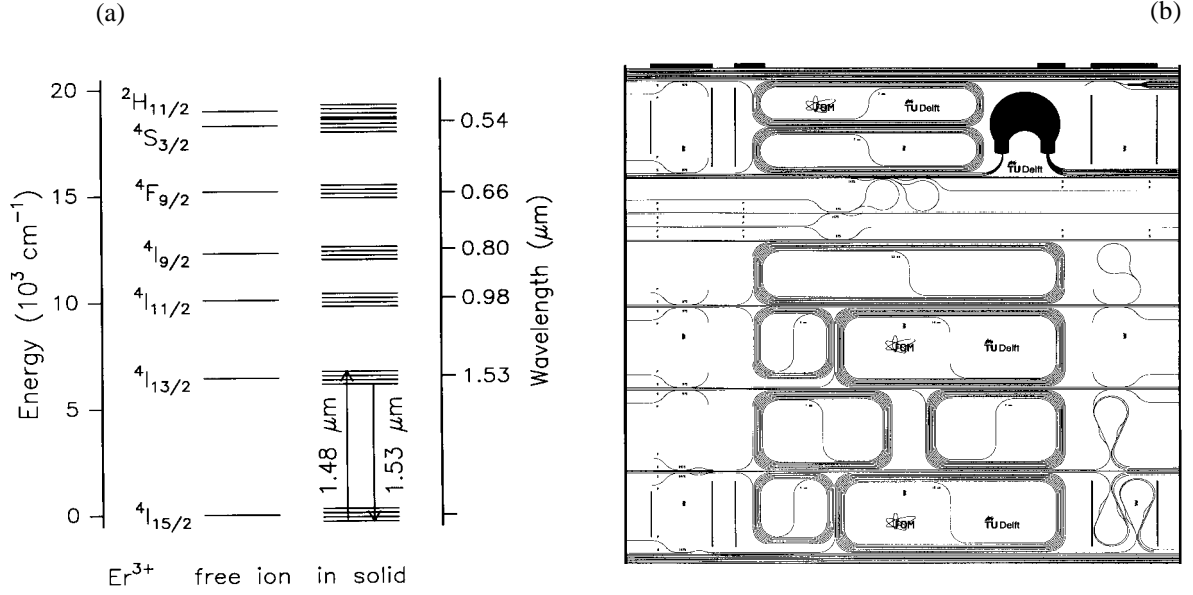


Fig. 1 (a) Energy level diagram of Er^{3+} . (b) Layout of a photonic integrated circuit. Straight channel waveguides, waveguide bends and loops, splitters, and wavelength division multiplexers are integrated on a single chip with an area of $1 \times 1 \text{ cm}^2$.

A schematic layout of an erbium-doped planar optical amplifier is shown in Fig. 2(a). Pump and signal beams are coupled into the device through separate input waveguides, and then combined in a wavelength division multiplexer (WDM). Next, an erbium-doped waveguide section is rolled up on a small area in the spiral structure (AMP), in order to combine long interaction length with small device area. After the AMP section, signal and pump are separated in a WDM, and a 1×4 splitter is added. The full device would then operate as a loss-free optical splitter. Note that the total device area is determined mostly by the size of the AMP spiral. Using a high-index waveguide core, waveguide bends as small as $50 \mu\text{m}$ can be made, and the spiral dimensions kept as small as 1 mm^2 . Note that such a small device could even be integrated in an optical fiber connector.

2. ER-DOPED OXIDE WAVEGUIDE AMPLIFIERS

2.1 Miniature Er-doped optical amplifier: an example

We have fabricated an Er-doped amplifier based on Al_2O_3 waveguide technology that was originally developed by Smit *et al.*⁵ To make these waveguides, a SiO_2 buffer layer is first grown on a Si substrate. Next a 600 nm -thick Al_2O_3 films is deposited by radio-frequency magnetron sputtering from an Al_2O_3 target. Er ions are then introduced in the film using ion implantation, and the waveguide layout (as in Fig. 2(a)) is defined using Ar atom beam etching. Finally, a SiO_2 cladding layer is deposited, and the in-and output facets are mechanically polished. Figure 2(b) shows an optical gain measurement on this structure in which a 4-cm long waveguide was doped with Er to a peak concentration of $0.3 \text{ at.}\%$.⁶ Using a 10 mW pump laser at $1.48 \mu\text{m}$, a gain at $1.53 \mu\text{m}$ of 4.0 dB is reached. Subtracting the waveguide loss for this particular waveguide, the net gain is 2.3 dB . This is the smallest Er-doped optical amplifier fabricated to date.

The measured pump power dependence of the optical gain was quite different than that predicted from the simple quasi-three-level scheme in Fig. 1(a), as indicated by the dashed line in Fig. 2(b). The reason is the occurrence of a non-linear process known as cooperative upconversion that significantly reduces the degree of Er population in the first excited state ($^4\text{I}_{13/2}$) at a given pump power.⁷ In this process, indicated schematically in Fig. 3(a), two excited Er ions exchange energy through a dipole-dipole interaction. As a result, one ion becomes de-excited to the ground state, while another one is excited to the $^4\text{I}_{9/2}$ level. The upconversion process must be included in the rate equation describing the de-population of Er in the first excited state:

$$\frac{dN_1}{dt} = -\frac{N_1}{\tau} - 2C_{up}N_{Er}N_1^2 \quad (1)$$

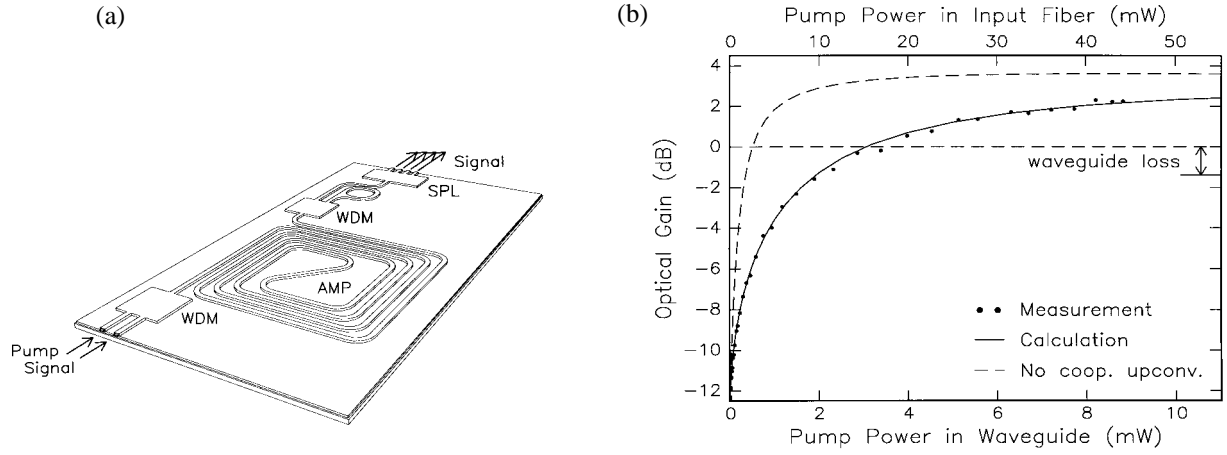


Fig. 2 (a) Schematic of miniature optical waveguide amplifier integrated with WDMs for pump and signal. (b) Optical gain measurement on an Er-implanted miniature optical amplifier based on Al_2O_3 . From van den Hoven *et al.*, Ref. 6.

with N_1 the population fraction in the first excited state, τ the lifetime for spontaneous emission from this level, N_{Er} the Er concentration, and C_{up} the upconversion coefficient. Upconversion is the main gain-limiting factor in planar optical amplifiers. In order to achieve high gain per unit length a high N_{Er} is required. At the same time, for a high N_{Er} , cooperative upconversion will cause the effective decay rate from the first excited state to increase (see Eqn. 1), and a higher pump power is required to achieve a certain degree of population inversion. For example, in Fig. 2(b), the pump power required to achieve net gain is 3 mW, while only 0.5 mW would be required if no upconversion took place.

2.2 Cooperative upconversion as the major gain limiting factor

The key parameter that must be measured on an Er-doped waveguide material before any predictions of possible gain can be made, is C_{up} . As an illustration of how this parameter can vary from material to material, we show in Fig. 3(b) an optical image of two identical waveguide spirals doped with the same N_{Er} of 0.3 at.%, both pumped at $1.48 \mu\text{m}$.⁸ The waveguide in the left-hand panel was doped by Er ion implantation, the one in the right-hand panel was fabricated by co-sputtering from a mixed $\text{Al}_2\text{O}_3/\text{Er}_2\text{O}_3$ target. The co-sputtered waveguide shows bright green emission (shown in white in the image), while the implanted waveguide shows only a faint green emission. The green originates from a second-order upconversion process, in which two Er ions that are first excited to the $^4\text{I}_{11/2}$ level through a first-order upconversion process interact, causing one of the two to become excited into the $^2\text{H}_{11/2}$ and $^4\text{S}_{3/2}$ levels, that emit in the green. The co-sputtered waveguide shows a dramatically higher upconversion than the implanted one, presumably because of clustering of Er or the formation of Er_2O_3 precipitates in the sputtered film. From measurements of the $^4\text{I}_{13/2}$ and $^4\text{I}_{11/2}$ level emission intensities as a function of pump power, measured in a channel waveguide, the upconversion coefficients for the two films were determined: $4 \times 10^{-18} \text{ cm}^3/\text{s}$ and $\approx 10^{-15} \text{ cm}^3/\text{s}$ for the implanted and sputtered films, respectively.⁸ Incorporating these numbers



Fig. 3 (a) Schematic of cooperative upconversion in Er^{3+} . (b) Optical images of two Al_2O_3 waveguides doped with Er to the same concentration (0.3 at.%) pumped at $1.48 \mu\text{m}$. Left: doped by ion implantation, Right: fabricated by $\text{Al}_2\text{O}_3/\text{Er}_2\text{O}_3$ co-sputtering. The green emission from the waveguides is represented in white. From Kik *et al.*, Ref. 8.

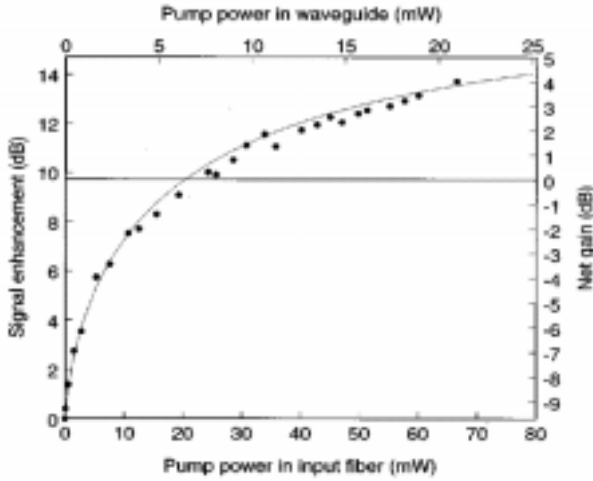


Fig. 4 Optical gain measurement at 1.53 μm on a 1-cm long Er-doped phosphosilicate glass waveguide amplifier on Si. A net gain of 4.1 dB is observed at a pump power of 21 mW. From Yan *et al.*, Ref. 11.

in Eqn. (1), the effective Er decay rate can be calculated for the two waveguides, assuming $N_{\text{Er}} = 0.3$ at.% Er, and 50 % inversion. The results are shown in Table I, together with the spontaneous decay rate for Er in Al_2O_3 in the case without upconversion. Clearly, a very high pump power is required to compensate for the increased decay rate in the sputtered film. The fabrication of Er-doped optical amplifier materials should therefore focus on atomic-scale engineering of the local environment and distribution of Er such that upconversion is minimized.

Table I: Er $^4\text{I}_{13/2}$ level decay rate in Al_2O_3 for three upconversion coefficients

	$^4\text{I}_{13/2}$ level decay rate (s^{-1})
no upconversion ($C_{\text{up}} = 0$)	130
Er implanted waveguide ($C_{\text{up}} = 4 \times 10^{-18} \text{ cm}^3/\text{s}$)	700
co-sputtered waveguide ($C_{\text{up}} = \approx 10^{-15} \text{ cm}^3/\text{s}$)	$\approx 10^5$

A parameter that is of key importance in determining whether net gain will be observed, given a known upconversion coefficient, is the mode confinement in the waveguide. Even for a relatively low upconversion coefficient, an Er excitation rate of order $>1000 \text{ s}^{-1}$ is required to achieve inversion (see Table I). At the typical Er absorption cross section of $3 \times 10^{-21} \text{ cm}^2$, this corresponds to a power density in the waveguide $> 50 \text{ kW}/\text{cm}^2$. In a well-confined waveguide with mode dimensions on the order of $1 \times 1 \mu\text{m}^2$, such as the Al_2O_3 structure shown above, this can be achieved at a pump power of a few mW. However, in a silica glass planar waveguide defined by e.g. an ion-exchange process with small index contrast, optical modes may be as large as $5 \times 5 \mu\text{m}^2$ and hence the pump power to reach inversion may well exceed 100 mW.^{9,10}

An example of a waveguide material that combines low upconversion with high index contrast is a multi-component phosphosilicate glass developed by Yan *et al.*¹¹ It is composed of Er_2O_3 , Al_2O_3 , Na_2O , La_2O_3 , and P_2O_5 . P_2O_5 -based glasses are known to be a good host for Er without clustering and indeed, the upconversion coefficient in this glass is only $2 \times 10^{-18} \text{ cm}^3/\text{s}$, the lowest value reported for a glass material. Na_2O is added as a network modifier, Al_2O_3 to increase the chemical resistance, and La_2O_3 to increase the refractive index ($n=1.535$). We have performed optical gain measurement (Fig. 4) on a 1 cm-long strip-loaded waveguide amplifier made in this glass and observed a net gain of 4.1 dB at 1.535 μm using 1.480 μm pumping at 21 mW. This is the highest gain per unit length measured on an Er-doped waveguide known to us.

2.3 Excited state absorption and the optimum amplifier length

One additional gain limiting factor in Er-doped amplifiers is excited state absorption (ESA), that occurs at high pump power, bringing an Er ion from the $^4\text{I}_{13/2}$ level into the $^4\text{I}_{9/2}$ level, by the absorption of a pump photon. The effect of ESA on the optical gain becomes significant when the higher lying states have appreciable lifetimes, leading to population built-up in levels that do not contribute to gain. As ESA depends on pump intensity, it becomes important when high pump powers are required, for example to compensate for the effect of upconversion. The effect of ESA is illustrated in Fig. 5(a), which shows a calculation of the Er population in a waveguide core consisting of a 2 μm wide, 520 nm thick ridge etched into a 800-nm thick Er-implanted Al_2O_3 film. The waveguide is pumped at 1.48 μm at a power of 100 mW. The Er population is plotted integrated over the thickness of the waveguide. The calculation takes into account the measured upconversion coefficient and Er absorption and emission cross sections, as well as the three-dimensional 1.48 μm pump and 1.53 μm signal mode distributions.¹² The dip in the center of the waveguide is due to ESA. The effect on the differential signal gain is seen in Fig. 5(b). It shows that at a pump power of 100 mW ESA causes a net signal loss. As the pump power decreases

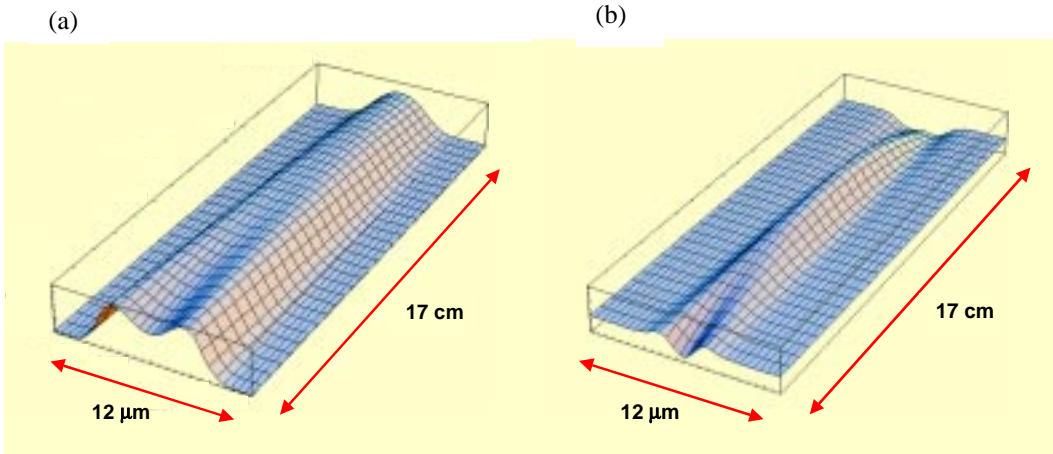


Fig. 5 (a) Degree of inversion and (b) differential gain along the length of the waveguide. Calculations are made for an Er-doped Al_2O_3 ridge waveguide, pumped at 100 mW at $1.48 \mu\text{m}$. The dip in the front facet is caused by excited state absorption. From Kik *et al.*, Ref. 12.

along the waveguide due to absorption (by Er and the waveguide structure) and scattering, the effect of ESA decreases and initially the differential gain increases. The differential gain becomes negative near the end of the waveguide due to the reduced pump intensity. The existence of an upper limit on the pump power shows that ESA puts a maximum to the length that can be used for a single-end pumped waveguide amplifier.

2.4 Enhancing the pump rate by Yb co-doping

One well-known technique to enhance the effective excitation efficiency of Er is by co-doping with ytterbium.¹³ As the $^2\text{F}_{5/2}$ level of Yb is resonant with the Er $^4\text{I}_{11/2}$ level, Yb→Er energy transfer can take place. This is then followed by a rapid non-radiative relaxation to the $^4\text{I}_{13/2}$ level in Er. As the absorption cross section of the Yb $^2\text{F}_{5/2}$ level (at 975 nm) is roughly tenfold higher than that of Er,¹⁴ this may cause an increased Er excitation rate. We have performed experiments on Er-doped Al_2O_3 waveguides fabricated by co-sputtering (0.3 at.% Er, see section 2.2) implanted with Yb (0.3 at.%), and measured the photoluminescence (PL) excitation spectrum as shown in Fig. 6.¹⁴ The Er $1.53 \mu\text{m}$ emission is measured as a function of pump wavelength in the 900-1020 nm spectral range for a sample with Er only and one co-doped with Yb. Clearly, the PL intensity in the Yb co-doped sample is enhanced by a factor ten. The spectral shape corresponds to the Yb absorption spectrum. From measurements of the decay time of the Yb emission at 975 nm we have also determined the Yb→Er energy transfer rate, it amounts to 2500 s^{-1} . It is important to realize that the energy transfer rate is determined by the Er concentration and distribution. It can not be increased by increasing the pump rate. Comparing the transfer rate with the numbers in Table I, it becomes clear that Yb sensitization is only useful in waveguides that have low upconversion.

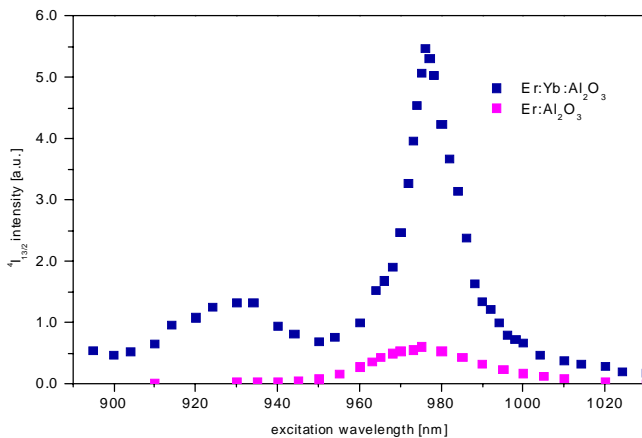


Fig. 6 PL excitation spectrum of Er and Yb co-doped Al_2O_3 . The Er $1.53 \mu\text{m}$ emission is measured as a function of pump wavelength. From Strohhöfer *et al.*, Ref. 14.

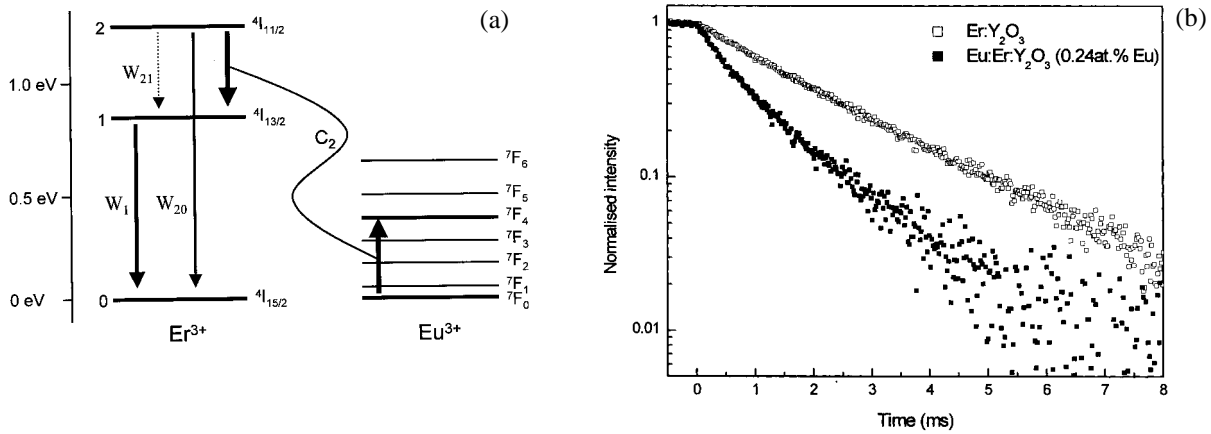


Fig. 7 (a) Schematic energy level diagram for energy transfer between Er and Eu. (b) PL decay measured at 980 nm (${}^4I_{11/2} \rightarrow {}^4I_{15/2}$ transition) in Er-implanted Y_2O_3 with and without Eu co-doping. From Strohhöfer *et al.*, Ref. 15.

2.5 Reducing upconversion by Eu co-doping

An alternative method to increase the efficiency of Er-doped planar amplifiers is by europium co-doping. As can be seen in the level diagram in Fig. 7(a), the ${}^7F_0 \rightarrow {}^7F_4$ transition in Eu is resonant with the ${}^4I_{11/2} \rightarrow {}^4I_{13/2}$ transition in Er. Therefore, energy transfer from Er to Eu can help to reduce the population of Er in the ${}^4I_{11/2}$ level, and to increase the population of the ${}^4I_{13/2}$ level that is used for amplification. This is particularly useful in amplifiers that are pumped at 980 nm, and which have a long luminescence lifetime of the ${}^4I_{11/2}$ level. The latter is typically the case in low-phonon energy materials such as e.g. Y_2O_3 . In Fig. 7(b) we show PL decay measurements of the 980 nm emission in Er^{3+} measured in a Y_2O_3 waveguide doped with 0.2 at.% Er (decay time 2.0 ms), and one co-doped with 0.25 at.% Eu (decay time 1.0 ms).¹⁵ The strong reduction in decay time is indicative of Er→Eu energy transfer that serves to reduce the ${}^4I_{11/2}$ population in the waveguide. Indeed, we found that the green upconversion in Er-doped Y_2O_3 waveguides is strongly reduced by Eu co-doping.¹⁵

2.6 Si quantum dots as a sensitizer for Er

Silicon quantum dots are known to absorb and emit light at wavelengths that are dependent on their size, due to a quantum confinement effect. We have fabricated Si nanocrystals in SiO_2 by Si ion implantation, followed by thermal annealing at 1100 °C.^{16,17} The quantum dot diameter ranges between 2–5 nm. Such quantum dots have absorption cross-sections as high as 10^{-14} cm^2 depending on the excitation energy and size.¹⁸ Next, we have doped these layers with Er by ion implantation with the aim to study the energy transfer between quantum dots and Er.¹⁹ Figure 8(a) shows a schematic of the energy bands involved. The nanocrystal bandgap is well above that of bulk Si (1.1 eV), while the Er ${}^4I_{15/2} \rightarrow {}^4I_{13/2}$ transition occurs at 0.8 eV.

Figure 8(b) shows a PL spectrum of a Si nanocrystal-doped layer implanted with a peak concentration of 1.8 at.% Er, measured at 300 K. The broad feature between 0.6 and 1.1 μm is due to the radiative recombination of quantum-confined excitons in nanocrystals that do not couple to Er. Two Er-related luminescence lines at 980 nm (${}^4I_{11/2} \rightarrow {}^4I_{15/2}$ transition) and 1.53 μm (${}^4I_{13/2} \rightarrow {}^4I_{15/2}$ transition) are also clearly distinguished. These PL spectra are measured under 458-nm excitation, a wavelength at which direct excitation of Er does not occur. In fact, PL excitation spectra clearly indicate that the Er is not excited directly into a 4f manifold, but rather indirectly, through the recombination of optically generated excitons in the nanocrystals. In this way the quantum dots act as efficient sensitizers for Er. From measurements as a function of temperature¹⁹ and Er concentration²⁰ we conclude that (1) the Er is excited through a strong coupling mechanism (i.e. a nanocrystal nearby an Er ion is optically dead), (2) the excitation rate at room temperature is $>10^6 \text{ s}^{-1}$, and (3) one nanocrystal can excite only 1-10 Er ions at a time.

An added advantage of the use of Si nanocrystals as sensitizers for Er is that they locally raise the refractive index and thereby create a waveguide. Figure 8(c) shows an intensity map of a 1.5 μm mode that was guided along a Si nanocrystal doped channel waveguide in SiO_2 . Excellent mode confinement is observed.²¹ Optical gain measurements in these waveguides are underway and a maximum gain of 1 dB/cm is predicted. If the nanocrystals could be excited electrically, it would become possible to fabricate an electrically pumped Er-doped optical amplifier.

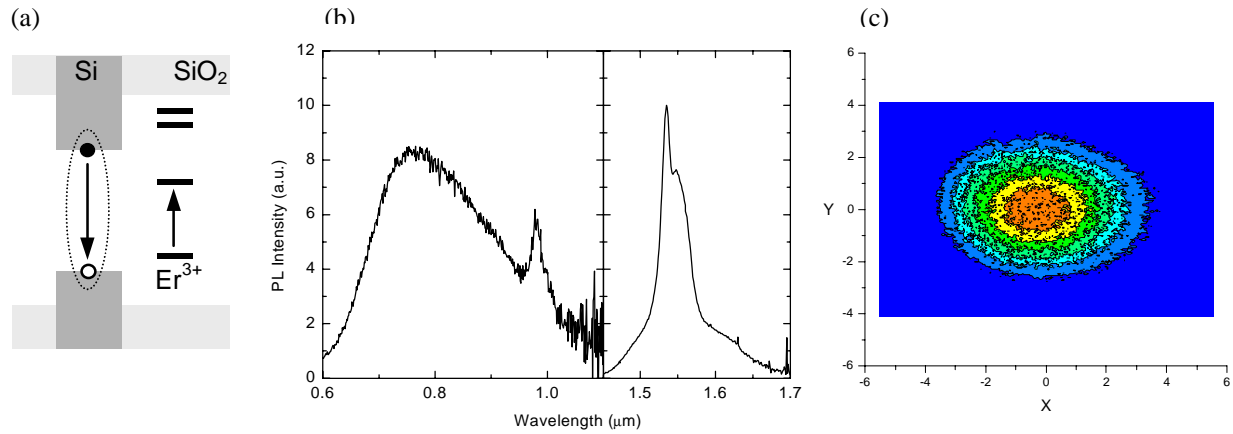


Fig. 8 (a) Schematic of energy levels involved in energy transfer between Si quantum dots and Er. (b) PL spectrum of Er-doped Si nanocrystal-doped SiO₂ measured at room temperature. Pump wavelength 458 nm. (c) Optical mode profile at 1.5 μm of a Si nanocrystal-doped channel waveguide in SiO₂. From Kik *et al.*, Refs. 19, 20, 21.

3. ER-DOPED POLYMER WAVEGUIDE AMPLIFIER MATERIALS

The importance of polymer optical waveguide technology is growing rapidly. First of all, polymer fibers are used more and more in short-distance optical links. Also, thin film integrated optical devices based on polymers become important. It would be of great interest to dope a polymer waveguide with Er in order to fabricate a polymer-based optical amplifier. Unfortunately, the erbium salts typically used in wet chemical processing are insoluble in the polymer precursors. To overcome this problem, we have studied two routes.

3.1 Er-doped organic cage complexes

We have designed a cyclic polydentate organic cage complex in which a rare earth ion is embedded (see Fig. 9(a)), that can be easily dissolved in a polymer matrix.^{22,23} In such a complex, the Er can be excited indirectly through the aromatic rings of the ligands that have a high absorption cross section. The Er luminescence spectrum is extremely broad, with a full width at half-maximum of 70 nm, enabling a high gain bandwidth.²² Unfortunately, the Er ions embedded in these complexes show large luminescence quenching, presumably due to coupling to vibrational states of the C–H bond in the complex itself, or O–H bonds in the solvents in which these complexes are processed. By selectively deuterating sections of the complex, and using deuterated solutions in the processing, the quenching can be slightly reduced,²⁴ but the highest luminescence lifetime at 1.53 μm, measured in DMSO-d₆ solution, is 5.4 μs, well below the estimated radiative lifetime of 4 ms.

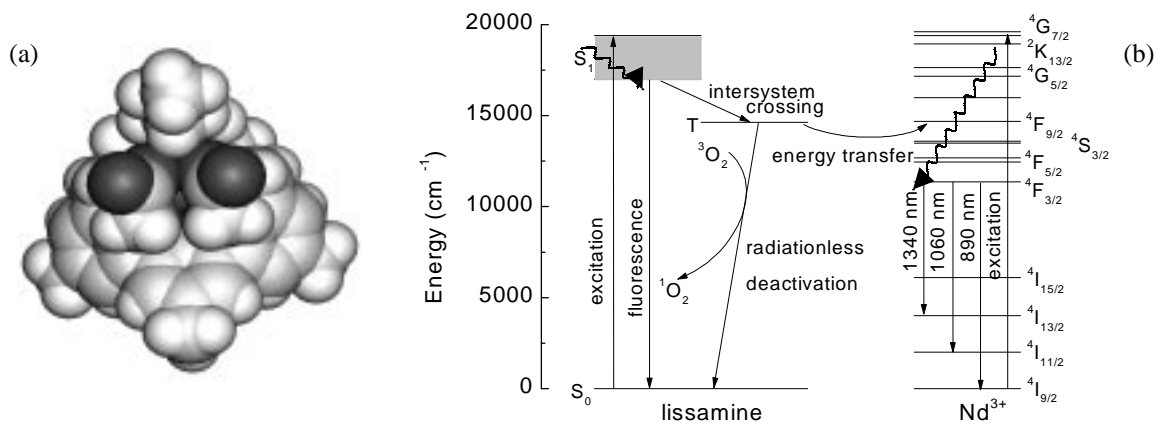


Fig. 9 (a) Schematic of cyclic polydentate organic cage complex in which a rare earth ion is embedded. (b) Energy transfer processes in a lissamine sensitized Nd-complex. From Slooff *et al.*, Refs. 22, 25 and Klink *et al.*, Ref. 23.

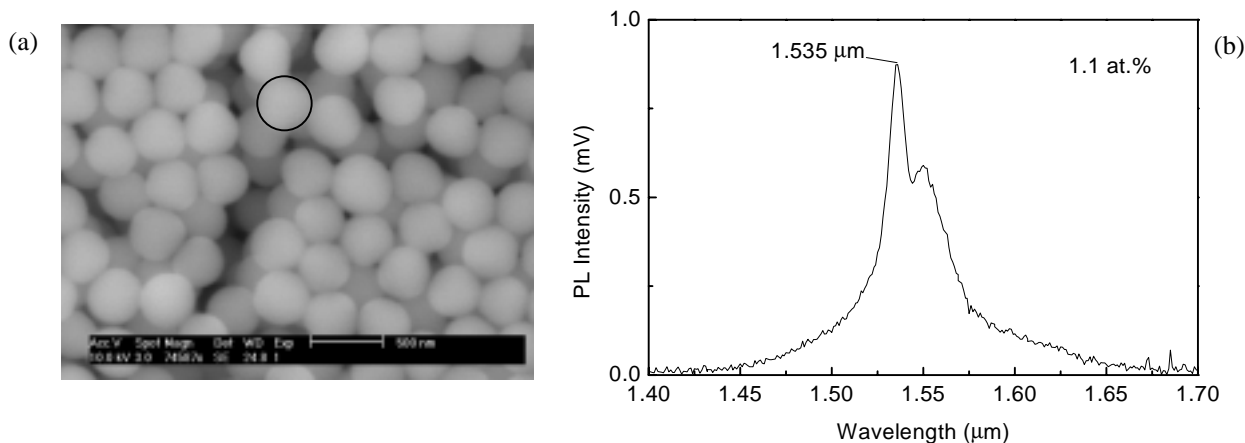


Fig. 10 (a) Scanning electron micrograph 360-nm diameter silica colloids deposited on a Si substrate. (b) PL spectrum of Er-implanted silica colloids, pumped at 488 nm From Slooff *et al.*, Ref. 27.

With such a high PL decay rate, very high pump powers are required to achieve inversion. To overcome this, a sensitizer can be attached to the complex, such as e.g. lissamine. Figure 9(b) shows the energy level diagram of a lissamine sensitizer, coupled to a Nd ion in a terphenyl-based complex.²⁵ The sensitizer can be excited very efficiently into the singlet state (cross section $>10^{-17}$ cm² at 500 nm). After rapid intersystem crossing to the triplet state, energy transfer can take place to the Nd ion, leading to excitation into the ⁴S_{3/2} and ⁴F_{9/2} levels. After relaxation to the ⁴F_{3/2} level, luminescence at 890, 1060, and 1340 nm is observed. The intramolecular energy transfer rate is as large as 10⁷ s⁻¹. These complexes can be embedded in a perfluorinated planar polymer waveguide with optical losses of 0.2 dB/cm at 1.5 μm.²⁵ Concentrations as high as 10 wt.% can be dissolved in the polymer. One problem in these waveguides is the strong photodegradation of the Nd luminescence that is observed upon continued optical pumping.²⁶ This photodegradation may be related to the presence of oxygen in the waveguide film, resulting in bleaching of the sensitizer. Such a problem could be overcome by using the proper steps in the waveguide processing.

3.2 Er-doped organic/inorganic nanocomposite waveguides

An alternative method to incorporate Er in a polymer waveguide is by using a nanocomposite material composed of Er-doped SiO₂ colloids embedded in a polymer. In this way the excellent properties of both materials: SiO₂ as a good host for Er, and the easy polymer processing, are combined. We have fabricated 360-nm diameter SiO₂ colloids by wet chemical processing using tetraethoxysilane (see Fig. 10(a)), and implanted them with Er to concentrations in the range 0.2–1.1 at.%.²⁷ Figure 10(b) shows a PL spectrum taken using excitation at 488 nm. PL lifetimes as high as 17 ms are observed, corresponding to a luminescence quantum efficiency as high as 80 %. The long lifetime is partly ascribed to the fact that the implanted colloids are mostly surrounded by air, with a low refractive index, and hence the local optical density of states in the colloids is relatively low, leading to a small radiative decay rate.²⁸ Optical gain calculations show that if these colloids could be embedded in a high-index-contrast waveguide with well-confined modes, an optical gain of 4 dB could be achieved for a 3-cm long waveguide at a pump power of only 10 mW. This calculation assumes an upconversion coefficient of 3×10⁻¹⁸ cm³/s, similar to that found for sodalime glass.⁹

4. ER-DOPED SILICON WAVEGUIDE AMPLIFIER MATERIALS

Silicon is one of the best known materials in the world. It is available in high purity and the processing technologies for silicon are by now very well established. While the properties of silicon as a semiconductor are well explored, it is not much used in photonic technology. However, Si is an excellent optical waveguide material, as it is completely transparent at 1.5 μm. If Si could be doped with high concentrations of optically active Er, an electrically pumped Er-doped amplifier could be made.

Figure 11(a) shows a schematic energy level diagram for Er-doped Si.²⁹ It resembles that for the Si nanocrystal-Er coupling scheme in Fig. 8(a), with the exception that the Si bandgap energy is now fixed at 1.1 eV, and that the exciton trapping takes place due to the presence of an Er-related defect state in the Si bandgap. As observed by many groups,³⁰ surface layers of single crystal Si doped with Er show clear Er-related PL at 1.53 μm under optical excitation at 488 nm. PL excitation

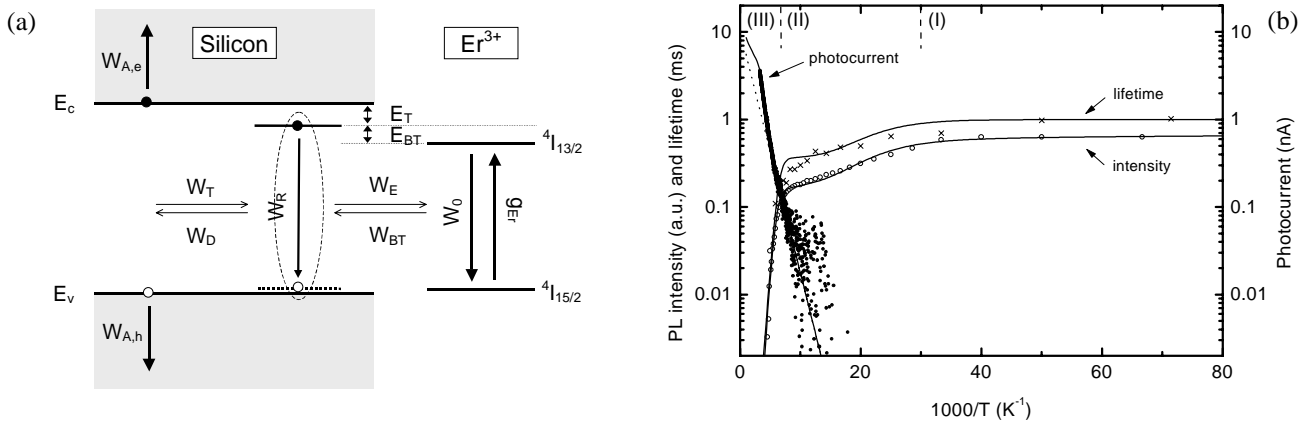


Fig. 11 (a) Schematic energy level diagram for Er-doped crystalline Si. (b) Arrhenius plot of the temperature dependence of 1.53 μm PL intensity and lifetime in Er-implanted Si p-n junction under optical excitation at 488 nm. Data for the 1.5 μm photocurrent are also included. From Hamelin *et al.*, Ref. 29.

spectroscopy shows that the excitation takes place in a three-step process in which (1) optically generated electron-hole pairs form an exciton trapped at the Er-related defect, (2) an impurity Auger process takes place in which the exciton recombines and energy is transferred to Er that then becomes excited into the $^4I_{13/2}$ level, and (3) the Er decays by the emission of a photon at 1.53 μm . Figure 11(b) shows the temperature dependence of the Er PL intensity and lifetime.²⁹ As can be seen, both show strong quenching at temperatures above 150 K. The quenching is mostly due to a backtransfer process, in which excited Er de-excites by the generation of the bound exciton state (W_{BT} in Fig. 11(a)). This may seem an improbable process, as it requires an additional 150 meV to bridge the gap between the Er $^4I_{13/2}$ energy and the exciton level, but as the PL lifetime of the $^4I_{13/2}$ state is very long (1 ms), this backtransfer process can actually be quite efficient. Eventually, the re-generated exciton may dissociate (W_T in Fig. 11(a)), leading to the generation of a free electron-hole pair that can be collected from a p-n junction. Temperature-dependent measurements of the 1.5 μm photocurrent of an Er-doped Si p-n junction are also included in Fig. 11(b).²⁹ Indeed, the photocurrent increases with temperature as expected for a phonon-assisted process. By fitting a rate-equation model to the three data sets in Fig. 11(b) we have identified all rate constants and activation energies in the diagram of Fig. 11(a).²⁹ We found that the internal quantum efficiency for the complete backtransfer process is as high as 70 % at room temperature. Er-doped Si waveguides could therefore serve as an infrared detector operating at 1.5 μm .

Several research groups have put significant effort in atomic-scale engineering of the Er site in Si such to minimize the quenching.^{31,32} It has been found that the addition of small concentrations of oxygen affects the local coordination for Er, and leads to smaller quenching. Indeed, weak room temperature PL of Er/O-doped Si has been observed both under optical and electrical excitation.³⁰ The challenge is now to further reduce this quenching and to increase the optically active fraction of Er. A fundamental problem that has been identified is the fact that Er can decay non-radiatively by an Auger process in which free carriers are excited high in the conduction/valence band.³³ Such carriers are provided by the Er itself, as Er (in particular in the presence of impurities such as O) shows donor behavior in Si. Efficient Er-doped Si waveguide amplifiers can therefore only be made if an Er site in Si is found that is optically active with small quenching, and at the same time is not (or only slightly) electrically active.

5. THE ULTIMATE MINIATURIZATION: PHOTONIC BANDGAP WAVEGUIDES

The size of a photonic integrated circuit is often determined by the smallest waveguide bending radius that can be made. For example, in the device layout of Fig. 1(b) for Al_2O_3 , the minimum radius is 50 μm . Thus, the total area of the amplifier spirals in Fig. 3(b) is 1 mm^2 . The radius could be further reduced by using a higher-index core material. Alternatively, a photonic bandgap effect may be used. As an example, we show our work on two-dimensional photonic crystals made of Si pillars. Figure 12(a) shows an array of 5 μm tall Si pillars, 205 nm in diameter, arranged in a square lattice with 570 nm pitch, made by deep anisotropic etching using an SF_6/O_2 electron cyclotron resonance driven plasma.³⁴ Optical bandstructure calculations for this structure are shown in Fig. 12(b) for TM and TE modes. A large bandgap (37 % of the

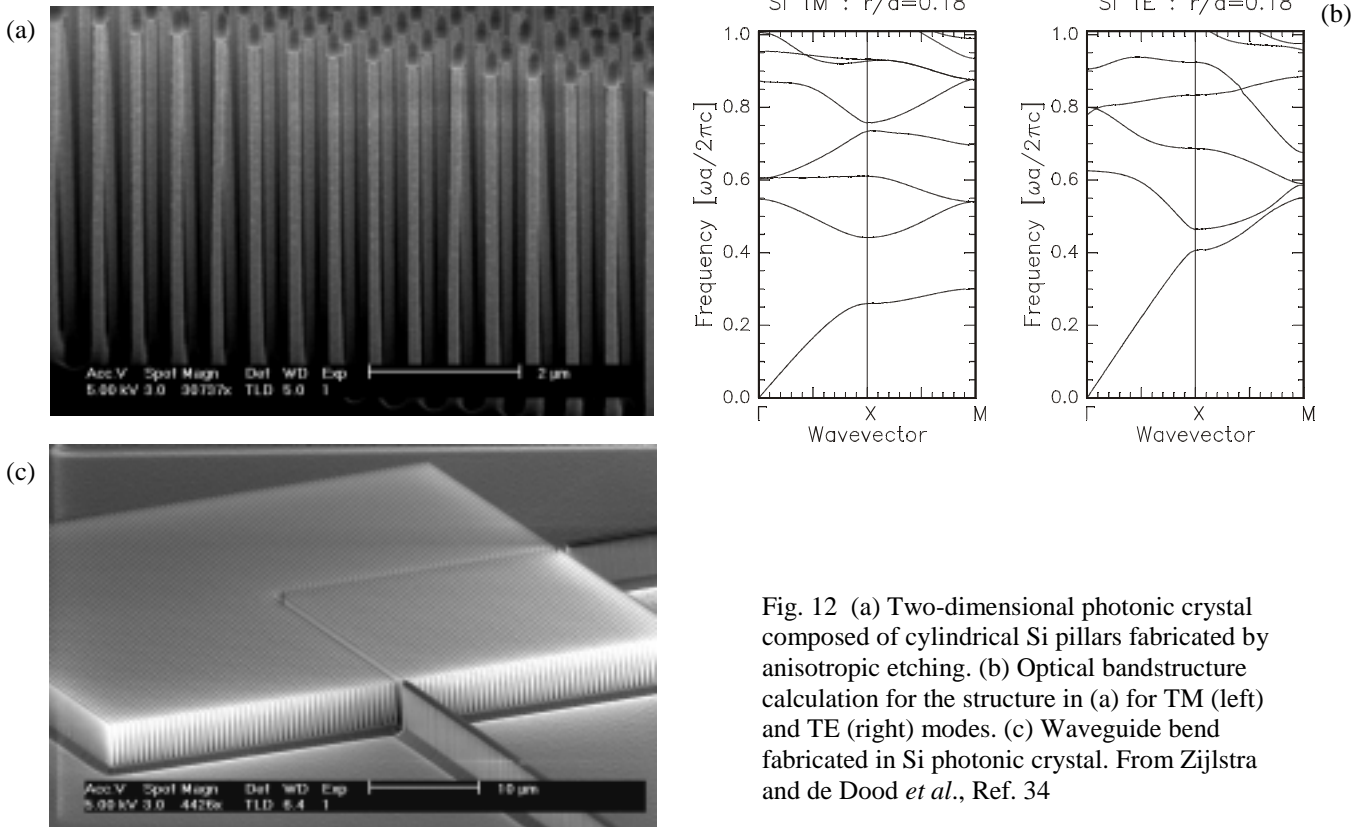


Fig. 12 (a) Two-dimensional photonic crystal composed of cylindrical Si pillars fabricated by anisotropic etching. (b) Optical bandstructure calculation for the structure in (a) for TM (left) and TE (right) modes. (c) Waveguide bend fabricated in Si photonic crystal. From Zijlstra and de Dood *et al.*, Ref. 34

central frequency) is observed for TM modes for our (pillar radius)/pitch ratio of 0.18. No bandgap is found for TE modes. For a pitch of 570 nm (as in Fig. 12(a)) the center gap for TM modes lies exactly at 1.53 μm. Figure 12(c) shows a waveguide bend that can be made using this material: an array of Si pillars is removed to define a waveguide in the pillar structure, in which otherwise no modes at 1.5 μm exist. In order to achieve confinement in the third dimension, a 2 μm thick region of the Si structure was amorphized before processing, using 4 MeV Xe irradiation. Input and output waveguides are integrated with the structure as can be seen in Fig. 12(c). Calculations predict an optical throughput as high as 98 % for the bend,³⁵ which has an effective radius of only 1.5 μm. Measurements on this device are underway. Note that photonic bandstructure effects may also be employed to suppress unwanted optical transitions, e.g. as occurring in upconversion processes described in section 2.

6. ACKNOWLEDGMENTS

This paper is a compilation of work performed by Pieter Kik, Lenneke Slooff, Christof Strohhofer, Michiel de Dood, Alfons van Blaaderen, Mark Brongersma, Nicholas Hamelin, Edwin Snoeks, and Gerlas van den Hoven at FOM-AMOLF, in collaboration with Frank van Veggel, Steve Klink and Gerald Hebbink at the Technical University Twente, Hans Hofstraat at AKZO NOBEL (now at Philips Research), Koos van Uffelen, Cor van Dam, Meint Smit, Tony Zijlstra and Emile van der Drift at the Technical University Delft, Martin Green at the University of New South Wales (Australia), Chris Buchal at Research Center Jülich (Germany), and Salvo Coffa at CNR-IMETEM (Catania). This work is part of the research program of the Foundation for Fundamental Research on Matter (FOM) and was made possible by financial support from the Dutch Foundation of Scientific Research (NWO), the IOP Electro-optics program of the Ministry of Economic affairs, the Dutch Technology Foundation (STW), and the Esprit Program of the European Union.

7. REFERENCES

- ¹ W.J. Miniscalco, "Erbium-doped glasses for fiber amplifiers at 1500 nm", *J. Lightwave Technol.*, p. 234, 1991
- ² E. Desurvire, *Erbium-doped fiber amplifiers: principles and applications*, John Wiley & Sons, 1994
- ³ S. Hüffner, *Optical spectra of transparent rear-earth compounds*, Academic, New York, 1978
- ⁴ see for a review of earlier work: A. Polman, "Erbium implanted thin film photonic materials", *J. Appl. Phys.* 82, p. 1, 1997.
- ⁵ M.K. Smit, *Integrated optics in silicon-based aluminium oxide*, Ph.D. Thesis, Delft University of Technology, 1991
- ⁶ G.N. van den Hoven, A. Polman, C. van Dam, J.W.M. van Uffelen, and M.K. Smit, "Net optical gain at 1.53 μm in Er-doped Al_2O_3 waveguides on silicon", *Appl. Phys. Lett.* 68, p. 1886, 1996
- ⁷ G.N. van den Hoven, E. Snoeks, A. Polman, C. van Dam, J.W.M. van Uffelen, and M.K. Smit, "Upconversion in Er-implanted Al_2O_3 waveguides", *J. Appl. Phys.* 79, p. 1258, 1996
- ⁸ P.G. Kik and A. Polman, to be published.
- ⁹ E. Snoeks, G.N. van den Hoven, A. Polman, B. Hendriksen, M.B.J. Diemeer, and F. Priolo, "Cooperative upconversion in erbium implanted sodalime silicate glass optical waveguides", *J. Opt. Soc. Am. B* 12, p. 1468, 1995
- ¹⁰ E. Snoeks, G.N. van den Hoven, and A. Polman, "Optimization of an Er-doped silica glass optical waveguide amplifier", *IEEE J. Quantum Electron.* 32, p. 1680, 1996
- ¹¹ Y.C. Yan, A.J. Faber, H. de Waal, P.G. Kik, and A. Polman, "Erbium-doped phosphate glass waveguide on silicon with 4.1 dB/cm gain at 1.535 μm ", *Appl. Phys. Lett.* 71, p. 2922, 1997
- ¹² P.G. Kik and A. Polman, to be published.
- ¹³ M.P. Hehlen, N.J. Cockroft, T.R. Gosnell, A.J. Bruce, "Spectroscopic properties of Er^{3+} - and Yb^{3+} -doped soda-lime silicate and aluminosilicate glasses", *Phys. Rev. B* 56, p. 9302, 1997
- ¹⁴ Ch. Strohhofer, P.G. Kik, and A. Polman, to be published
- ¹⁵ Ch. Strohhofer, P.G. Kik, and A. Polman, "Selective modification of the $\text{Er}^{3+} {}^4\text{I}_{11/2}$ branching ratio by energy transfer to Eu^{3+} ", submitted to *J. Appl. Phys.* 2000
- ¹⁶ K.S. Min, K.V. Shcheglov, C.M. Yang, H.A. Atwater, M.L. Brongersma and A. Polman, "Defect-related versus excitonic visible light emission from ion beam synthesized Si nanocrystals in SiO_2 ", *Appl. Phys. Lett.* 69, p. 2033, 1996
- ¹⁷ M.L. Brongersma, P.G. Kik, A. Polman, K.S. Min, and H.A. Atwater, "Size dependent electron-hole exchange splitting in Si nanocrystals", *Appl. Phys. Lett.*, 76, p. 351, 2000
- ¹⁸ D. Kovalev, J. Diener, H. Heckler, G. Polisski, N. Künzer, and F. Koch, "Optical absorption cross sections of Si nanocrystals", *Phys. Rev. B* 61, p. 4485, 2000
- ¹⁹ P.G. Kik, M.L. Brongersma, and A. Polman, "Strong exciton-erbium coupling in Si nanocrystal doped SiO_2 ", *Appl. Phys. Lett.*, 76, 2000, in press
- ²⁰ P.G. Kik, and A. Polman, "Maximum excitable Er concentration in Si nanocrystal-doped SiO_2 ", submitted to *J. Appl. Phys.*, 2000
- ²¹ P.G. Kik and A. Polman, to be published.
- ²² L.H. Slooff, A. Polman, M.P. Oude Wolbers, F.C.J.M. van Veggel, D. Reinhoudt, and J.W. Hofstraat, "Optical properties of erbium-doped polydentate organic cage complexes", *J. Appl. Phys.* 83, p. 497, 1998
- ²³ S.I. Klink, G.A. Hebbink, L. Grave, F.C.J.M. van Veggel, D.N. Reinhoudt, L.H. Slooff, A. Polman, and J.W. Hofstraat, "Sensitized near-infrared luminescence from polydentate triphenylene-functionalized Nd^{3+} , Yb^{3+} , and Er^{3+} complexes", *J. Appl. Phys.* 86, p. 1181, 1999
- ²⁴ G.A. Hebbink *et al.*, to be published
- ²⁵ L.H. Slooff, A. Polman, S.I. Klink, G.A. Hebbink, L. Grave, F.C.J.M. van Veggel, D.N. Reinhoudt, and J.W. Hofstraat, "Optical properties of lissamine functionalized Nd^{3+} complexes in polymer waveguides and solution", *Optical Materials* 14, p. 101, 2000.
- ²⁶ L.H. Slooff, A. Polman, S.I. Klink, G.A. Hebbink, L. Grave, F.C.J.M. van Veggel, D.N. Reinhoudt, and J.W. Hofstraat, to be published
- ²⁷ L.H. Slooff, M.J.A. de Dood, A. van Blaaderen, and A. Polman, "Erbium-implanted silica colloids with 80 % luminescence quantum efficiency", submitted to *Appl. Phys. Lett.*, 2000
- ²⁸ E. Snoeks, A. Lagendijk, and A. Polman, "Measuring and modifying the spontaneous emission rate of erbium near an interface", *Phys. Rev. Lett.* 74, p. 2460, 1995
- ²⁹ N. Hamelin, P.G. Kik, J.F. Suyver, K. Kikoin, A. Polman, A. Schönecker, and F.W. Saris, "Energy backtransfer and infrared photocurrent in erbium-doped silicon p-n junctions", submitted to *J. Appl. Phys.* 2000

-
- ³⁰ See for a review: “Light emission from Er-doped Si: Materials properties, mechanisms, and device performance”, S. Coffa, G. Franzò, and F. Priolo, *MRS Bulletin* 23/4, p. 25, 1998
- ³¹ J. Michel, J.L. Benton, R.F. Ferrante, D.C. Jacobson, D.J. Eaglesham, E. Fitzgerald, Y.-H. Xie, and L.C. Kimerling, “Impurity enhancement of the 1.54 μm Er^{3+} luminescence in silicon”, *J. Appl. Phys.* 70, p. 2667, 1991
- ³² F. Priolo, G. Franzò, S. Coffa, A. Polman, S. Libertino, R. Barklie, and D. Carey, “The erbium-impurity interaction and its effect on the 1.54 μm luminescence of Er^{3+} in silicon”, *J. Appl. Phys.* 78, p. 3874, 1995
- ³³ F. Priolo, G. Franzò, S. Coffa, and A. Carnera, “Excitation and nonradiative deexcitation processes of Er^{3+} in crystalline Si”, *Phys. Rev. B* 57, p. 4443, 1998
- ³⁴ T. Zijlstra, E.W.J.M. van der Drift, M.J.A. de Dood, E. Snoeks, and A. Polman, “Fabrication of two-dimensional photonic crystal waveguides at 1.5 μm in silicon by deep anisotropic etching”, *J. Vac. Sci. Technol. B* 17, p. 2734, 1999
- ³⁵ A. Mekis, J.C. Chen, I. Kurland, S. Fan, P.R. Villeneuve, and J.D. Joannopoulos, *Phys. Rev. Lett.* 77, p. 3787, 1996